Separation Science and Technology
Publication details, including instructions for authors and subscription information:
http://www.informaworld.com/smpp/title~content=t713708471

Effects on Gas Chromatographic Peaks of Electric Fields Applied across Cholesteric Liquid Crystal Stationary Phases

J. E. Conaway[a]; L. B. Rogers[a]
[a] DEPARTMENT OF CHEMISTRY, UNIVERSITY OF GEORGIA, ATHENS, GEORGIA

To cite this Article Conaway, J. E. and Rogers, L. B.(1978) 'Effects on Gas Chromatographic Peaks of Electric Fields Applied across Cholesteric Liquid Crystal Stationary Phases', Separation Science and Technology, 13: 4, 303 — 320
To link to this Article: DOI: 10.1080/01496397808057104
URL: http://dx.doi.org/10.1080/01496397808057104

SEPARATION SCIENCE AND TECHNOLOGY, 13(4), pp. 303-320, 1978

Effects on Gas Chromatographic Peaks of Electric Fields Applied across Cholesteric Liquid Crystal Stationary Phases

J. E. CONAWAY and L. B. ROGERS

DEPARTMENT OF CHEMISTRY
UNIVERSITY OF GEORGIA
ATHENS, GEORGIA 30602

Abstract

Earlier studies have shown that a static electric field across a capillary column increased the apparent capacity ratio (measured from the peak maximum) of a liquid crystal stationary phase and produced a more nearly Gaussian-shaped peak plus a small step on the front of the peak. The present study has qualitatively confirmed those effects using cholesteryl laurate, cholesteryl 10-undecenoate, and cholesteryl benzoate, and suggests that they may be found for all cholesteric liquid phases. In addition, the peak-fronting phenomenon was found to be a function of both the carrier gas and the applied column potential. Fragmentation of the solute and/or the stationary phase by carrier gas molecules in metastable excited states is proposed to explain the fronting phenomenon. Hysteresis effects have also been observed, indicating that the liquid crystals may take hours to return to their original orientations after imposition or removal of an electric field.

INTRODUCTION

Electric fields have been used by several workers (*1–3*) to modify the chromatographic behavior of liquid crystal stationary phases coated on glass capillary columns. Changes were reported in capacity factors calculated from peak maxima and in peak shapes. When high-precision gas chromatography (*3–6*) was used, an additional effect of an electric field, a small step at the leading edge of the peak, was discovered (*3*).

The primary objective of the present work was to investigate the generality of those effects using cholesteryl laurate, cholesteryl 10-undecenoate, and cholesteryl benzoate. In addition, more information has been obtained about the fronting phenomenon mentioned above.

EXPERIMENTAL

Reagents

Cholesteryl benzoate, cholesteryl 10-undecenoate (Vari-Light Corp.) and cholesteryl laurate (Eastman Kodak) were used as received. Chloroform and dichloromethane (J. T. Baker, reagent grade) were used as solvents to make up solutions of the liquid crystals for coating the capillary columns.

Acetone (J. T. Baker, reagent grade), *n*-pentane, cyclopentane, cyclohexane (Matheson, Coleman, and Bell, spectroquality), and *n*-hexane (Phillips Petroleum 99% mol. pure) were used as volatile solutes. All solutes were stored over 4Å molecular sieve and used without further purification.

Methane (Selox, Inc.) was used as a "nonretained" solute. Hydrogen and compressed air (Selox, Inc.) were used for the flame ionization detector. Carrier gases were helium, argon, and nitrogen (Selox, Inc.). All gases were passed through silica gel and 4Å molecular sieve traps. In addition, helium was also passed through a diffusion cell (Electron Technology, Inc., Model SLM–1A) for further purification before use in some experiments.

Apparatus

The gas chromatograph has been described earlier (*3*, *6*) except for the following changes. A Brooks electronic mass flow controller (Model 5810–1N3D4A, solenoid Model 5835–A2C4D) was used for the carrier gas. Brooks (Model 8743) and Porter (Model VCD–100) mechanical flow controllers were installed on the compressed air and hydrogen lines, respectively, in conjunction with rotameters so as to improve detector stability. An unregulated variable high voltage power supply was constructed to give 0 to 680 V to be applied across the column.

The data acquisition system was the same as that described earlier (*3*, *6*). All signals from the electrometer were first fed into an amplifier system consisting of a low-drift operational amplifier (Analog Devices, Model 184L) and a chopper-stabilized operational amplifier (Analog Devices, Model 232J). The amplifier output was measured by an autoranging multichannel analog-to-digital converter (Anscan, Model 3700, Beckman Instruments). The digitized chromatogram was then processed and stored on magnetic tape by a PDP 11/20 mini-computer (Digital Equipment Company, Maynard, Massachusetts). All computer programs were written in BASIC modified by a real-time overlay (*7*).

Procedures

All capillary columns were constructed of borosilicate glass as described earlier (*1–3*). In brief, a wire (No. 36 gauge Chromel A, Hoskins Mfg. Co., Detroit, Michigan) was pulled through the center of the capillary as it was being drawn.

The capillary columns were coated as previously described using the usual dynamic method (*1–3*). After dissolving the liquid crystal in the appropriate solvent, a stream of dry nitrogen was used to push the coating solution through the column at approximately 2 cm/sec.

After the inside surface had been coated with the stationary phase, the outer surface of the capillary was coated with a graphite paste and covered with aluminum foil for electrical continuity. Some physical characteristics of the capillary columns are given in Table 1.

The columns were conditioned for 12 hr at 10°C above the isotropic transition temperature using helium gas at a flow of 5 cc/min. Columns were then installed in the chromatograph oven as described earlier (*3*, *6*) using shrinkable Teflon tubing (Alltech Associates, Arlington Heights, Illinois) for connection to the detector and to the sampling valve. Low vapor pressure epoxy cement (Torr-Seal, Varian Inc., Palo Alto, California) was used to seal the connection where the internal wire exited the column.

The procedures for operating the chromatograph have been described earlier (*3*, *6*). After an initial period in which the carrier gas flow was

TABLE 1

Capillary Column Characteristics

Column	Stationary phase	Length (m)	Effective radius (mm)	Coating solution
1	Cholesteryl laurate	38	0.19	0.60 g/1.5 ml CH_2Cl_2
2	Cholesteryl benzoate	16	0.20	0.50 g/ml $CHCl_3$
3	Cholesteryl 10-undecenoate	30	0.17	0.48 g/ml $CHCl_3$

allowed to stabilize, methane was injected to determine the retention time of a nonretained species. When carriers other than helium were used, the flow rate was adjusted to give the same retention time for methane. Experiments with and without applied potential followed using the solute of interest. A 22-port valve (Valco Instrument Co., Houston, Texas) was used to select one of the five solutes. Injection was accomplished by first bubbling helium through a saturator filled with solute and then charging up an exponential dilution flask prior to opening the sampling valve. However, on the basis of earlier work (*2*, *3*) and our preliminary studies, acetone was chosen as the solute for detailed examination of changes in peak shape with potential.

The temperature of the gas chromatographic oven was chosen on the basis of the mesomorphic range of the liquid crystal used: cholesteryl laurate, 77 to 89°C; cholesteryl benzoate, 148 to 176°C; and cholesteryl 10-undecenoate, 66 to 78°C (*1*, *8*, *9*). In general, the temperature was set at approximately the middle of that range. The compartment for the flame ionization detector (FID) was heated to 350°C using a cartridge heater to avoid condensation. The detector temperature was monitored using an iron–constantan thermocouple.

The electric field was applied by connecting the positive and negative terminals of the high-voltage power supply to the wire and aluminum foil, respectively. The high-voltage power supply and the sample injection valves were switched on simultaneously in those experiments in which an electric field was to be applied.

In experiments where only the column current was to be measured, the chromatographic operating conditions were the same as usual, except that no injection of solute was made. A digital multimeter (Keithley, Model 160) was connected in series with the high-voltage power supply for these measurements.

Data acquisition was performed as previously described (*3*, *6*) with 200 data points being taken across the methane peak and 230 points across a solute peak. Retention times of both methane and the solute were first determined using a strip-chart recorder (Sargent, Model SRL) to determine an approximate delay period prior to the beginning of computer data acquisition. Delay periods and data acquisition rates were varied so as to have at least two-thirds of the points taken after the peak maximum in order to include most of the tail. In general, the acquisition rate varied from 2.5 to 10 Hz following a corresponding delay period of 180 to 30 sec.

Calculations

The zeroth through the second moments were calculated using the appropriate summations (*10*). The average linear flow rate was calculated from

$$\bar{\mu} = L/t_0 \tag{1}$$

where $\bar{\mu}$ is the average linear flow of carrier gas, L is the column length, and t_0 is the time for the methane peak.

Peak maxima were determined simply by the location of the maximum data point. Due to the asymmetry of the peaks, polynomials were not fitted across the top of the peak. The relative changes in peak maxima were calculated using the relationship

$$\%\Delta M = 100\left(\frac{T_v - T_0}{T_0}\right) \tag{2}$$

where $\%\Delta M$ is the percent change in the peak maximum, T_v is the solute retention time with an applied potential of v volts, and T_0 is the solute retention time with no applied potential.

The effective column radii were calculated from the relationship (*3*, *11*)

$$\sigma = \sqrt{8\bar{\mu}\eta L/\Delta P} \tag{3}$$

where σ is the column radius, $\bar{\mu}$ is the average linear velocity of the carrier gas, η is the carrier gas viscosity, L is the column length, and ΔP is the pressure drop across the column.

RESULTS

Peak Maxima and Means

In order to investigate the generality of the invariance of the first moment with applied potential reported for cholesteryl myristate (*3*), we chose to study a column coated with a structurally similar liquid crystal, cholesteryl laurate. Figure 1 shows two chromatograms of acetone obtained for the cholesteryl laurate column, one with no applied potential and another at 300 V applied potential. The latter showed both a shift to a longer maximum-based retention time and the production of a more nearly Gaussian-shaped peak. Although the peak maxima for the two chromatograms were different, their first moments were very similar (Table 2), indicating no change in thermodynamic behavior resulting from the application of a field.

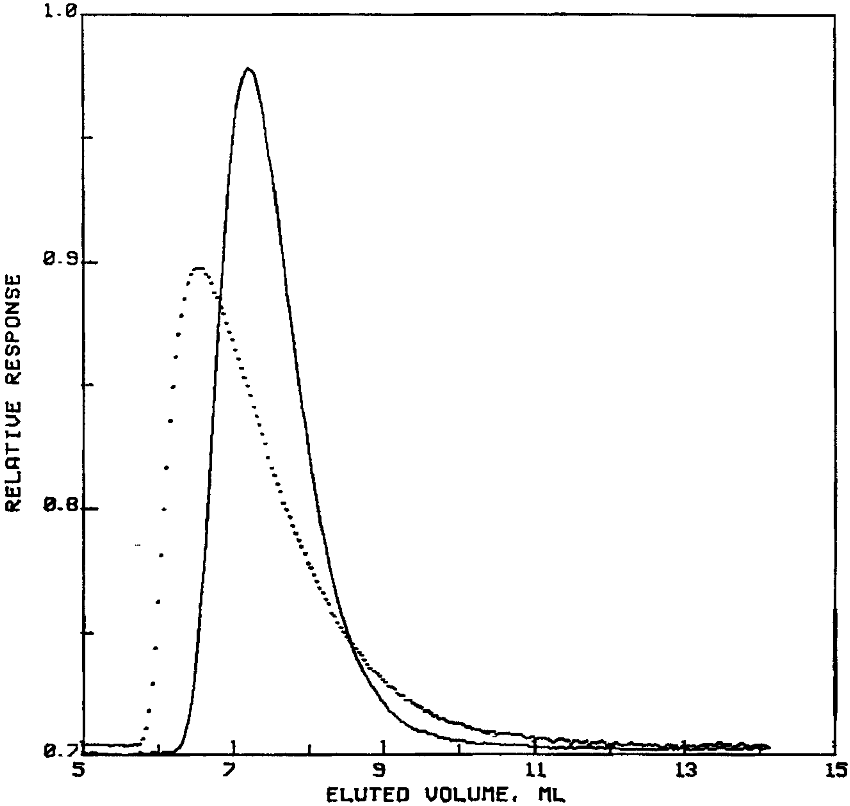

FIG. 1. Effect of 300 V potential on peak shape for acetone on cholesteryl laurate at 82 °C and an average linear velocity of 19 cm/sec: (··) 0 V and (—) 300 V.

TABLE 2

Effects on Peak Moments of Acetone on Cholesteryl Laurate of 300 V Applied Potential

	Peak moments		
Applied potential (V)	0th	1st	2nd
0	2.14×10^7	266.23	1465.43
300	2.12×10^7	266.24	566.29

To determine the effect of structural differences on chromatographic behavior of the stationary phase, the relative shift in maximum-based retention time versus applied potential was examined for cholesteryl laurate and cholesteryl benzoate. The results of repeated injections of acetone with nitrogen carrier gas at successively higher potentials on both columns are shown in Fig. 2. Each data point represents the average of three values; range bars represent standard deviations. Both liquid crystals showed comparable shifts in peak maxima with potential under similar conditions. Although only two data points are shown for cholesteryl benzoate, they followed the same trend as those for cholesteryl laurate.

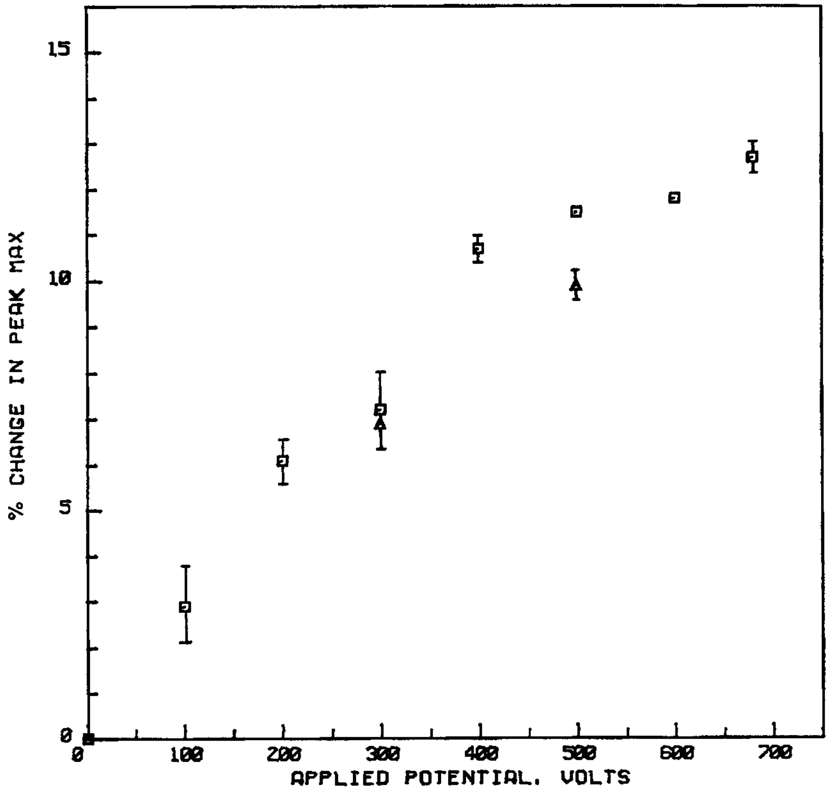

Fig. 2. Effect of potential on the relative shift in maximum-based retention time for acetone on two liquid crystal columns at average linear velocities of 39 cm/sec: (▣) cholesteryl laurate, 82 °C, and (△) cholesteryl benzoate, 154 °C.

The scatter in the data was probably due to the highest data point being used for the maximum-based retention time. Barring noise spikes, the time resolution was limited by the data acquisition rate.

Fronting

Cholesteryl laurate, cholesteryl 10-undecenoate, and cholesteryl benzoate were used as stationary phases, and helium, nitrogen, and argon as carrier gases. A series of 0.5 μl injections of helium saturated with acetone vapor was made onto the cholesteryl benzoate column at various applied potentials using helium as a carrier gas. All chromatograms in Fig. 3 were recorded at the same sensitivity. Note first that a shift to longer retention times occurred as the potential was increased from 0 to 300 V. Due to the rapid flow rate in this experiment, however, any narrowing of the peak was imperceptible. Second, at 400 V a shoulder occurred on the leading edge of the peak and the height of the parent peak was greatly diminished. At 450 V the shoulder was evolving into a peak equal in height to the parent peak, and at 500 V only the shoulder remained. Third, increasing the potential above 300 V caused an increasing baseline drift. This effect was most apparent in the chromatogram obtained at 500 V. Similar behavior was obtained on both cholesteryl laurate and cholesteryl 10-undecenoate columns under similar chromatographic conditions.

Neither the fronting phenomenon nor the baseline drift was observed when nitrogen or argon was used as a carrier gas even though all other conditions remained the same. For that reason, several experiments were performed to determine why helium (or its impurities) produced this behavior. Figure 4 shows current–voltage curves obtained on the cholesteryl laurate column. Both argon and nitrogen showed relatively small currents compared to helium at potentials above 300 V. The ultrapure helium obtained from the diffusion cell showed slightly higher currents compared to helium purified by the more conventional method using silica gel and molecular sieve traps. This slight difference could be due to impurities that were removed by the diffusion cell.

Similar results for both the trends in the current–voltage curves and the differences between the gases were obtained for a cholesteryl 10-undecenoate column at 74 °C, as shown in Fig. 5. In addition, a large temperature effect was noticed when the experiment was repeated at 94 °C. As shown by Fig. 6, the currents for all three carrier gases increased dramatically, although both ultrapure and conventional helium still deviated in behavior from argon and nitrogen.

In order to explore whether or not the production of metastable excited-state helium atoms could in some way be responsible for the fronting, the baseline drift, and the large column currents, a small amount of methane, as a quench gas, was leaked into the helium before it passed through the cholesteryl laurate column. Figure 7 shows that the addition of methane reduced the currents for helium to values not unlike those obtained with either argon or nitrogen.

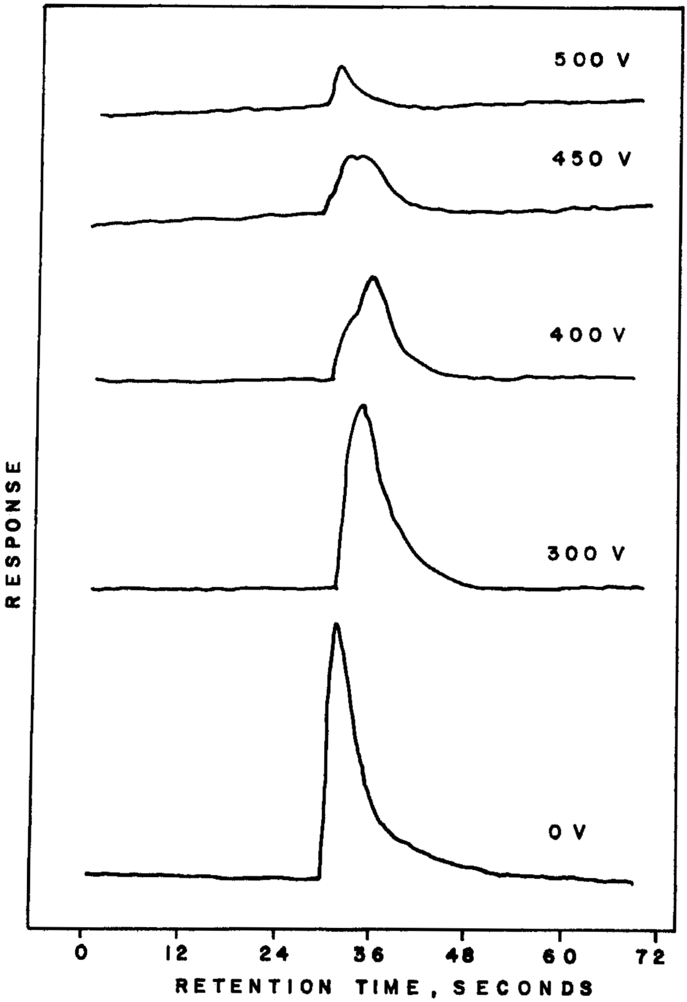

FIG. 3. Effect of potential on peak fronting for acetone on cholesteryl benzoate at 154°C.

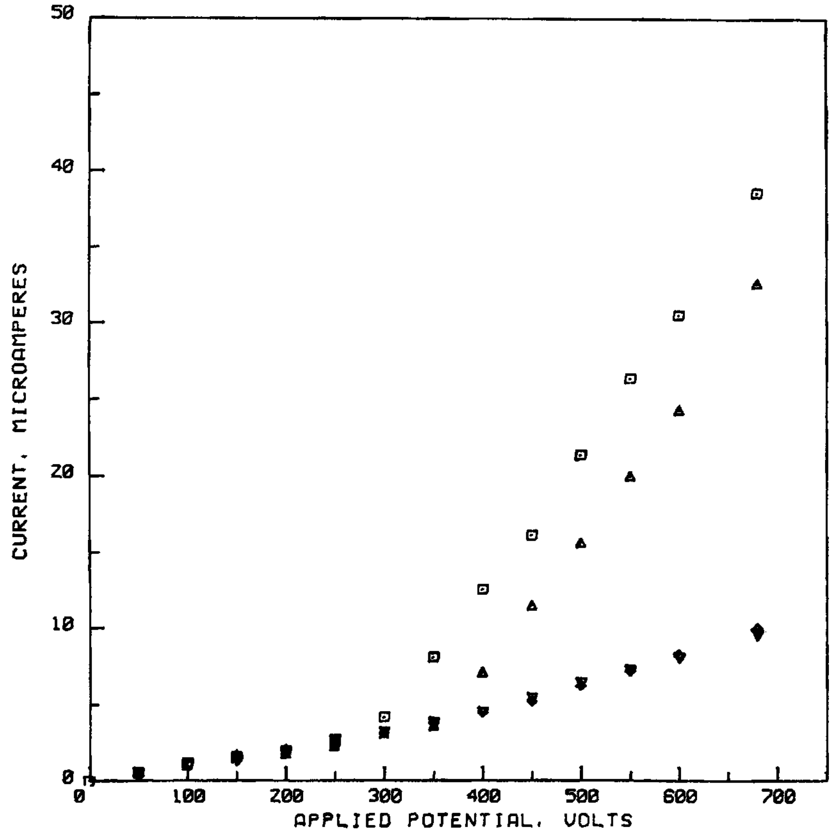

FIG. 4. Column current as a function of applied potential on cholesteryl laurate at 82 °C: (▣) helium carrier gas purified by diffusion cell, (△) helium carrier gas, (▽) nitrogen carrier gas, and (◇) argon carrier gas.

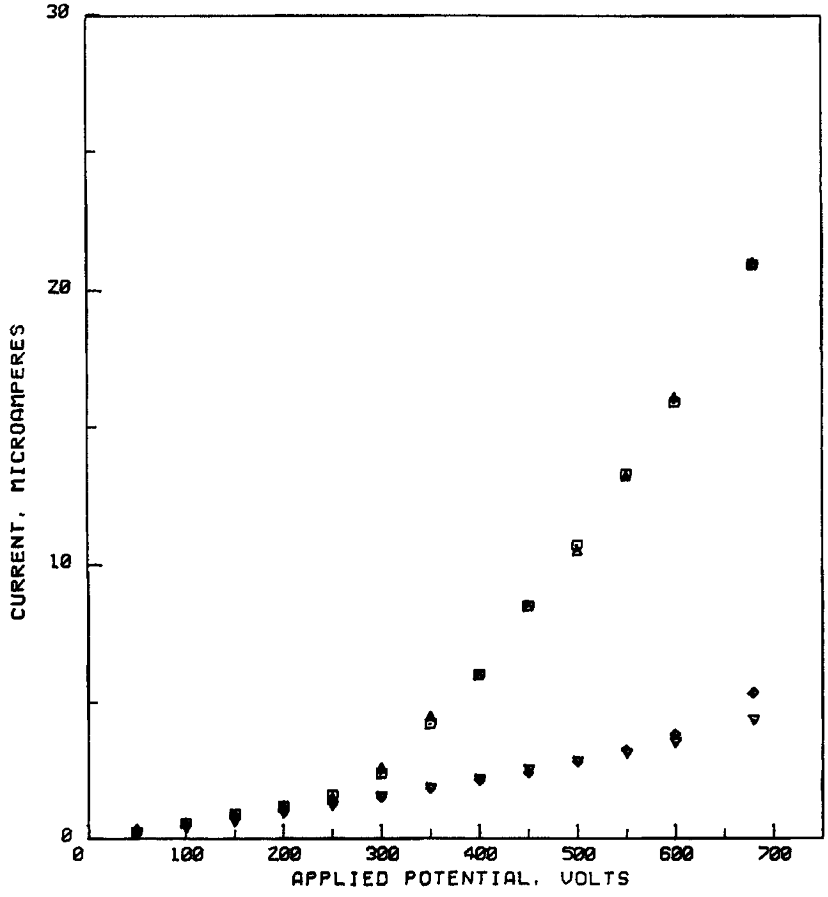

FIG. 5. Column current as a function of applied potential on cholesteryl 10-undecenoate at 74°C: (◬) helium carrier gas purified by diffusion cell, (▣) helium carrier gas, (◈) argon carrier gas, and (▽) nitrogen carrier gas.

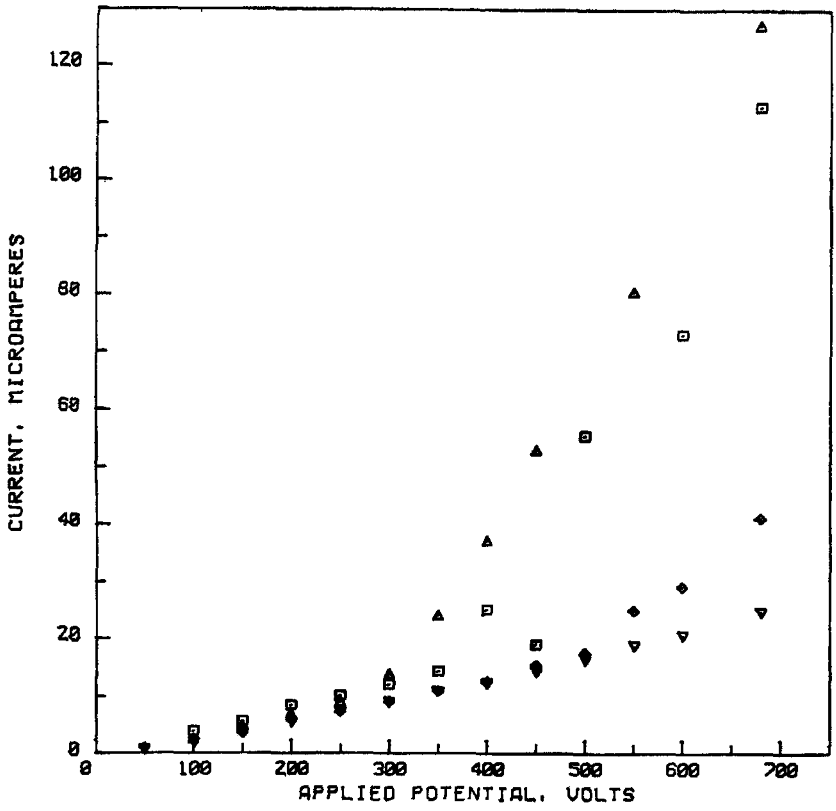

FIG. 6. Column current as a function of applied potential on cholesteryl 10-undecenoate at 94 °C: (△) helium carrier gas purified by diffusion cell, (▣) helium carrier gas, (◇) argon carrier gas, and (▽) nitrogen carrier gas.

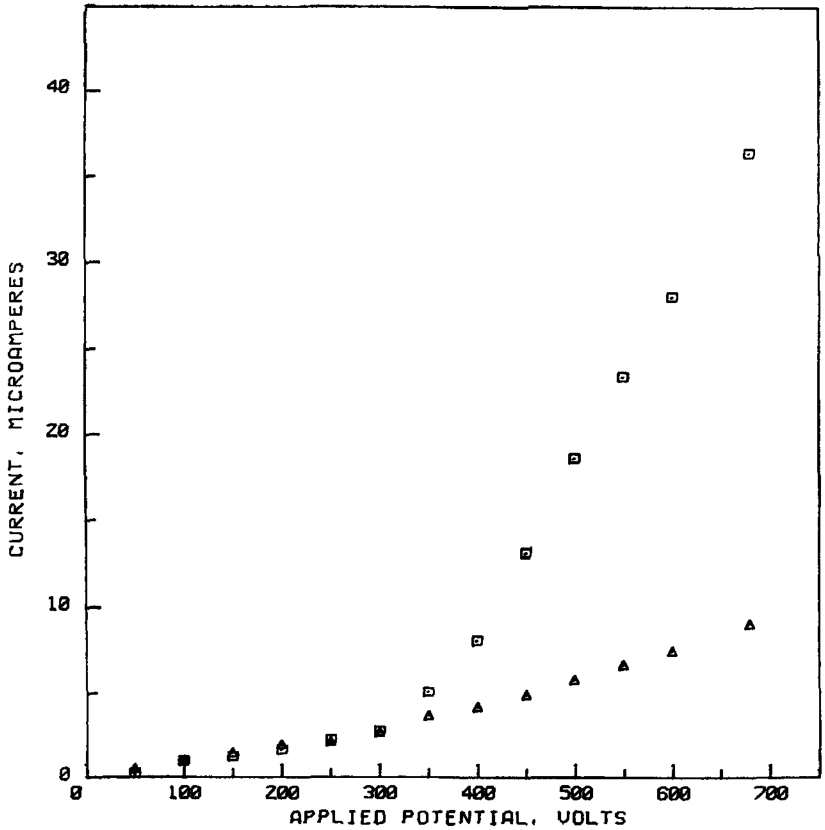

FIG. 7. Effect on column current of adding methane to helium on cholesteryl laurate at 82°C: (▣) helium carrier gas purified by diffusion cell, and (△) helium carrier gas with methane added.

Hysteresis Effects

During the course of this study we noted that, following a period during which a large potential had been applied, there was not an immediate return to the original "no-potential" retention time for the maximum. Instead, a period of approximately 24 hr was usually required, presumably to permit the liquid crystals to return to their original random orientations. Similarly, repeated application of a moderate potential for repeated injections of acetone on the cholesteryl laurate column resulted in a gradual decrease with time in the second moment of the peak, as shown by Fig. 8. Hence application of a moderate potential did not cause immediate align-

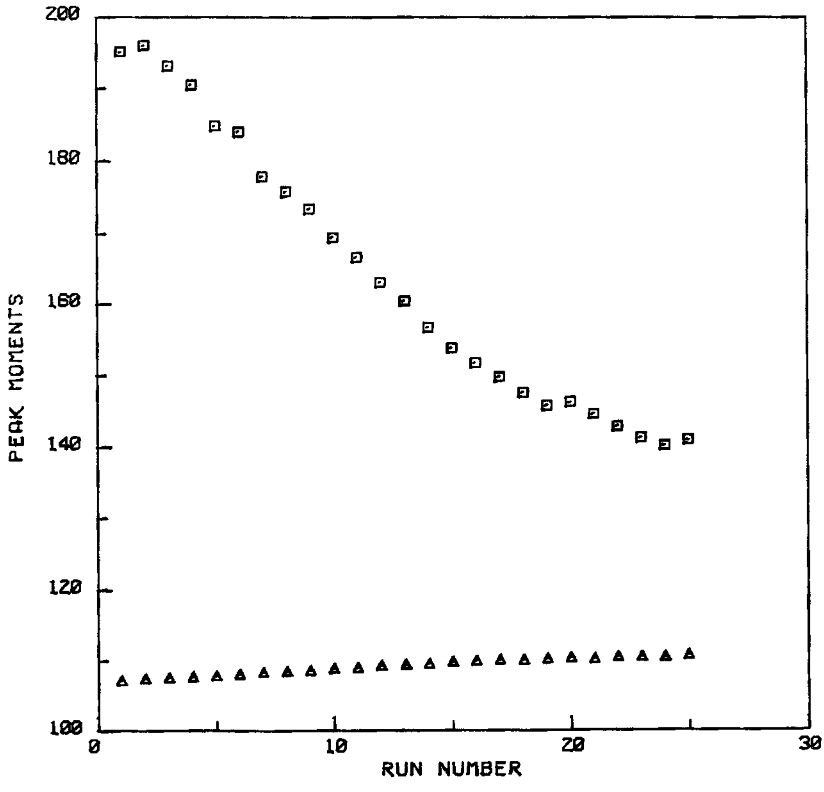

FIG. 8. Effect on peak moments of repeated injections of acetone on cholesteryl laurate at 200 V applied potential: (▲) first moment, and (▣) second moment.

ment of the liquid crystal molecules, just as removal of the field failed to result in an immediate return to a random orientation.

CONCLUSIONS

Since both the cholesteryl laurate and cholesteryl benzoate columns yielded comparable shifts in peak maxima, structural differences between the two ester groups were obviously not critical. This is not surprising since the shifts in peak maxima are, for the most part, due probably to changes in the resistance to mass transfer in the stationary phase with applied potential (*3*) rather than to a decrease in film thickness or geometrical rearrangement. The lowering of the resistance to mass transfer with applied potential is probably due, in turn, to a field-induced convective movement within the stationary phase.

The fronting phenomenon, which was reported earlier for cholesteryl myristate using several different solutes (*3*), has been observed for three additional liquid crystals. Furthermore, fronting occurred only above 300 V when helium was the carrier gas. These observations are consistent with the large column currents and the baseline drift, both of which were observed above 300 V when helium was the carrier gas. This implies that two interactions were occurring within the liquid crystal columns: one with the stationary phase molecules, as evidenced by the large measured currents and baseline drift, and one with the solute molecules, as shown by the fronting.

Earlier workers attributed the fronting observed on cholesteryl myristate to the production of a more volatile species by breakdown of the solute and stationary phase under the influence of the electric field (*3*). This seems to be consistent with our results. Furthermore, helium seems to be involved in the process. Direct ionization of the carrier gas by the electric field seems unlikely since helium has the highest first ionization potential and metastable state energy of the three carrier gases, as shown by Table 3

TABLE 3

First Ionization Potentials and Metastable State Energies for Various Carrier Gases

Gas	1st ionization potential (eV) (*12*)	Metastable state energy (eV) (*13*)
He	24.48	20.6
N_2	15.15	11.8
Ar	15.75	11.7

(*12*, *13*). The fact that an addition to helium of a polyatomic species, such as methane, reduced the measured currents substantially, as shown in Fig. 7, suggests that metastable excited-state helium atoms were produced within the column and were then interacting with molecules of both the solute and the stationary phase.

That explanation is patterned after the one that takes place in proportional counters used for detection of nuclear radiation. The addition of a polyatomic organic gas to a noble gas such as helium quenches the metastable species through collisional deactivation and prevents discharge within the tube (*14*, *16*).

However, the production of metastable excited-state helium atoms is not entirely consistent with our observations. Since helium has the highest metastable state energy, it is the most difficult of the three gases to excite to a metastable state. One would therefore expect to see similar behavior for all three carrier gases if this process were occurring. It is possible that either an impurity was present in both the argon and the nitrogen in sufficient quantity to quench any metastable species, or that the metastable energies of argon and nitrogen were insufficient to ionize the organic species present in the column. The second possibility, though, seems highly unlikely. Furthermore, the effect of temperature on measured currents on cholesteryl 10-undecenoate, shown by Figs. 5 and 6, also tended to disprove production of metastable excited-state helium atoms as the sole mechanism accounting for our observations. Production of metastable species should be fairly temperature independent, since any energy from thermal contributions should be negligible compared to the excitation energies involved. The observed temperature effect suggests a second temperature-dependent step following the initial production of metastable species.

It is also possible that the dielectric properties of the carrier gas are responsible in part for the phenomena we have observed. Table 4 shows the permittivity, molar polarization, and polarizability of helium, argon, nitrogen, and methane at 20°C and atmospheric pressure (*17*). The relationship between these quantities for nonpolar gases at moderate temperature and pressure is given by the Clausius-Mossotti equation:

$$P = \frac{E_0 - 1}{E_0 + 2}\frac{M}{d} = \frac{4}{3}\pi N\alpha \qquad (4)$$

where P is the total molar polarization, E_0 is the permittivity of the gas, M is the molar mass of the gas, d is the gas density, N is Avogadro's number, and α is the polarizability of the gas (*17*, *18*). The values in

TABLE 4

Dielectric Properties of Helium, Argon, Nitrogen, and Methane

Gas	$10^6(E_0 - 1)$	P (cm^3)	$10^{24}\alpha$ (cm^3)
Helium	65.0	0.521	0.21
Argon	517.2	4.146	1.64
Nitrogen	548.0	4.394	1.74
Methane	—	6.53	2.59

Table 4 show simply that helium deviates from argon, nitrogen, and methane in that it has a much lower "insulating ability." It is therefore possible that the dielectric properties of the gases contributed to the behavior we have observed.

Unfortunately, our observations do not allow an unambiguous mechanism to be proposed for the phenomena. Further examination of the phenomena using mass spectrometry should provide more detailed information regarding the mechanism.

The hysteresis effects reported here show that the liquid crystals did not immediately assume either an aligned or a random configuration. This behavior is not unexpected since the liquid crystals were in the mesomorphic range where they still possessed some restrictions on molecular movement. One would expect the effects to be less noticeable at temperatures in the isotropic range. At any rate, these effects suggest that care must be taken when using electric fields for alignment of liquid crystals in order to allow adequate time for equilibration of molecular orientation within the field. For this reason we attempted either to allow adequate time for equilibration or to keep a constant time interval between experiments that were performed at successively higher potentials.

Acknowledgments

This study was supported in part by a Fellowship from Tennessee Eastman Company (JEC) and in part by the U.S. Energy Research and development Administration Contract No. E(38–1)–854.

Helpful discussions with Joaquin Lubkowitz of the Instituto Venezolano de Investigaciones Cientificas are gratefully noted.

REFERENCES

1. P. J. Taylor, R. A. Culp, C. H. Lochmüller, L. B. Rogers, and E. M. Barrall, II, *Sep. Sci.*, *6*, 841 (1971).
2. P. J. Taylor, A. O. Ntukogu, S. S. Metcalf, and L. B. Rogers, *Ibid.*, *8*, 245 (1973).

3. R. B. Westerberg, F. J. Van Lenten, and L. B. Rogers, *Ibid.*, *10*, 593 (1975).
4. M. Goedert and G. Guiochon, *Anal. Chem.*, *42*, 969 (1970).
5. J. E. Oberholtzer and L. B. Rogers, *Ibid.*, *41*, 1234 (1969).
6. F. J. Van Lenten, J. E. Conaway, and L. B. Rogers, *Sep. Sci.*, *12*, 1 (1977).
7. J. E. Davis and L. B. Rogers, *Real-Time Overlay for 1-8 User BASIC-11*, Decus Program Library, Decus No. 11-95, 1973.
8. Vari-Light Corporation, *Vari-Light High Purity Cholesterol Esters*, Cincinnati, Ohio 45242.
9. Eastman Kodak Co., *Eastman Liquid Crystal Products*, Kodak Publication No. JJ-14, 1973, p. 17.
10. S. N. Chesler and S. P. Cram, *Anal. Chem.*, *43*, 1922 (1971).
11. L. S. Ettre, *Open Tubular Columns in Gas Chromatography*, Plenum, New York, 1965, pp. 38–40.
12. *Handbook of Chemistry and Physics*, Chemical Rubber Company, Cleveland, 1972, pp. E56, E62.
13. J. Sev̌cik, *Detectors in Gas Chromatography*, Elsevier, Amsterdam, 1976, p. 69.
14. P. Rice-Evans, *Spark, Streamer, Proportional and Drift Chambers*, Richilieu, London, 1974, pp. 42, 98.
15. W. J. Price, *Nuclear Radiation Detection*, 2nd ed., McGraw-Hill, New York, 1964, pp. 123–124.
16. P. J. Ouseph, *Introduction to Nuclear Radiation Detectors*, Vol. 2, Plenum, New York, 1975, pp. 74–76.
17. N. E. Hill, *Dielectric Properties and Molecular Behavior*, Van Nostrand Reinhold, New York, 1969, p. 192.
18. W. J. Moore, *Physical Chemistry*, 4th ed., Prentice-Hall, Englewood Cliffs, New Jersey, 1972, pp. 700–702.

Received by editor June 21, 1977